

## Cloning, Expression, and Characterization of a Thioredoxin Reductase cDNA from *Taiwanofungus camphorata*

CHIH-YU HUANG,<sup>†,||</sup> CHUIAN-FU KEN,<sup>‡,||</sup> HSIANG-HUI CHI,<sup>†,||</sup> LISA WEN,<sup>§,||</sup> AND  
 CHI-TSAI LIN<sup>\*†</sup>

<sup>†</sup>Institute of Bioscience and Biotechnology and Marine Center for Bioscience and Biotechnology, National Taiwan Ocean University, Keelung 202, Taiwan, <sup>‡</sup>Institute of Biotechnology, National Changhua University of Education, Changhua 500, Taiwan, and <sup>§</sup>Department of Chemistry, Western Illinois University, 1 University Circle, Macomb, Illinois 61455-1390. <sup>||</sup>These authors contributed equally to this paper.

A cDNA encoding putative thioredoxin reductase (TR) was identified from a medicinal mushroom, *Taiwanofungus camphorata* (*T. camphorata*). Alignment of the deduced amino acid sequence with TRs from other organisms showed high levels of identity (59–74%). A three-dimensional (3-D) homology structure was created for this TR. Functional *T. camphorata* TR (TcTR) was overexpressed in yeast and purified. The purified enzyme showed a monomeric form on a 10% sodium dodecyl sulfate–polyacrylamide gel electrophoresis (SDS–PAGE). The enzyme's half-life of deactivation at 60 °C was 12.9 min, and its thermal inactivation rate constant  $K_d$  was  $5.37 \times 10^{-2} \text{ min}^{-1}$ . The optimal pH for the enzyme was pH 8 and retained about 76% activity in the presence of 0.1 M imidazole. The enzyme showed 50% activity after 10 min of incubation at 37 °C with chymotrypsin. The Michaelis constant ( $K_m$ ) value for dithionitrobenzoate (DTNB) was 1.59 mM.

**KEYWORDS:** *Taiwanofungus camphorata*; three-dimensional (3-D) homology structure; thioredoxin reductase (TR); dithionitrobenzoate [DTNB, 5-5-dithiobis(2-nitrobenzoic acid)]; thioredoxin (Trx)

### INTRODUCTION

The main function of thioredoxin reductase (TR) is to catalyze the reduction of a multifunctional thioredoxin (Trx) and of numerous other oxidized cell constituents. The reduced dithiol-containing Trx [Trx(SH)<sub>2</sub>] is a potent protein disulfide reductase, while the oxidized disulfide Trx [TrxS<sub>2</sub>] is regenerated by TR in a NADPH-dependent manner. Trx has been reported to act as a growth factor of various cell types and tumor cell lines (1). Trx also plays an important role in the antioxidant defense of cells (2). Mitsui et al. (3) reported that overexpression of human Trx in transgenic mice resulted in protection against oxidative stress and a possible extension of life span. Trx has been proposed to play a key role in controlling the oxidative state of crucial cysteine residues that mediates the induction of genes involved in the oxidative stress (oxidative stress in cells is a state in which ROS levels exceed the available antioxidant defenses) response. Thus, TR plays very important roles in maintaining Trx and other cellular constituents in their reduced form. TR is an FAD containing enzyme involved in the transfer of hydrogens from Trx to other proteins such as peroxyredoxin (Prx), thus providing a disulfide reductase system.

TRs belong to a family of glutathione reductase-like homodimeric flavoenzymes. There are two families of TRs: (1) The

35 kDa (subunit) TRs occurring in prokaryotes, fungi, and plants (4, 5) and (2) the 55 to 60 kDa (subunit) TRs that have been identified in *Plasmodium falciparum*, *Drosophila melanogaster*, and mammals (6, 7). The high molecular weight TRs have a C-terminal peripheral redox center that can communicate with the central redox-active catalytic site (8). TR and Trx have been shown to play a pathophysiological role in chronic diseases such as rheumatoid arthritis and certain malignancies. The effects of antitumor drugs such as cisplatin and carmustine can be explained in part by the inhibition of TR, and high levels of the TRs can be linked to drug resistance (2).

Nature has historically been a rich source of structurally diversified bioactive compounds. Plant and fungal extracts can provide highly potent bioactive ingredients having unique structural properties. In Asia, medicinal mushrooms believed to increase longevity in traditional practice have long been regarded as health foods. *Taiwanofungus camphorata* (formerly named *Antrodia camphorata*, also known as “niu-chang-chih” or “niu-chang-ku” in Taiwan) is a unique medicinal mushroom species found only in the forests of Taiwan which uses *Cinnamomum kanehirai* hay as its host. *Antrodia camphorata* was first published using the name *Ganoderma camphoratum*, a mistake due to contamination of spores of a *Ganoderma* species (9). The species was described as *Antrodia cinnamomea* by Chang and Chou (10). Wu et al. (11) confirmed that both specimens of *G. camphoratum* and *A. cinnamomea* are conspecific and proposed new combination: *Antrodia camphorata* (11). A phylogenetic analysis based on the sequence data of rRNA genes of a large ribosomal subunit indicated that

\*To whom correspondence should be addressed. Institute of Bioscience and Biotechnology, National Taiwan Ocean University, 2 Pei-Ning Rd., Keelung 202, Taiwan. Phone: 886-2-24622192 ext. 5513. Fax: 886-2-24622320. E-mail: B0220@mail.ntou.edu.tw.

*A. camphorata* is distantly related to other species in *Antrodia* (12). The fungus was transferred to the new genus *Taiwanofungus* (12). However, *A. camphorata* was reconsidered as an *Antrodia* species after polymorphism analysis of internally transcribed spacer regions of the rRNA gene (13).

*Taiwanofungus camphorata* is a well-known traditional Chinese medicine used to treat liver diseases, cancer, food and drug intoxication, abdominal pain, and itchy skin (14, 15). Historically, *T. camphorata* was used in Taiwan by the native Taiwanese to treat discomforts caused by drinking alcohol or fatigue. Although *T. camphorata* shows physiological activities with great potential in medical applications, little is known about the exact bioactive compounds of the mushroom, and many bioactive ingredients are yet to be discovered. Recently, we established the EST (expressed sequence tag) from fruiting bodies of *T. camphorata* in order to search active components for possible health food applications. We have cloned and characterized several antioxidant enzymes including a 1-Cys peroxiredoxin (16), a novel 2-Cys peroxiredoxin (17), a cambialistic-superoxide dismutase (18), a catalase (19), a glutathione-dependent formaldehyde dehydrogenase (20), a phospholipid hydroperoxide glutathione peroxidase (21), a dithiol glutaredoxin (22), and a 2-Cys peroxiredoxin isozyme (23). Here, we report the first cloning and expression of a reduction enzyme, TR cDNA, from *T. camphorata*. The coding region of the cDNA was introduced into a *Saccharomyces cerevisiae* expression system. The functional target protein was overexpressed, purified, and its properties studied.

## MATERIALS AND METHODS

**Total RNA Preparation from *Taiwanofungus camphorata* and cDNA Synthesis.** Fruiting bodies of *T. camphorata* grown in the hay of *C. kanehirai* were obtained from the central part of Taiwan. Fresh fruiting bodies (wet weight 5 g) were frozen in liquid nitrogen and ground to powder in a ceramic mortar. The mRNA (15  $\mu$ g) was obtained using Straight A's mRNA Isolation System (Novagen). Three micrograms of the mRNA was used for 5'-RACE-Ready cDNA and 3'-RACE-Ready cDNA synthesis using Clontech's SMART RACE cDNA Amplification Kit.

**Isolation of TcTR cDNA.** Using 5'-RACE-Ready cDNA of *T. camphorata* as a template and two degenerate primers (5'GAA AAY TTY CCH GGB TTY CC 3' and 5'GCW CCR TCR CAH ACR GCA CA 3'), a 0.3 kb fragment was amplified by PCR. The degenerate primers were designed on the basis of the conserved sequences of TR from *S. pombe* (EMBL accession no. AAN01228), *S. cerevisiae* (EMBL accession no. P38816), and *A. thaliana* (EMBL accession no. Q39242). The 0.3 kb fragment was subcloned and sequenced. On the basis of this DNA sequence, two primers near both ends, a TR-9 primer (5'CGC GAA ACT TGT CCA TCA AC 3') and a TR-8 primer (5'GTT TGA AGG GTG AGG AGA CG 3'), were synthesized. The primers allowed sequence extension from both ends of the 0.3 kb fragment when used with the UPM primer (universal primer A mix, purchased from BD biosciences). Two PCRs were carried out each using 0.1  $\mu$ g of the 5'-RACE-Ready cDNA or 3'-RACE-Ready cDNA as a template. The primer pairs in each reaction were UPM and TR-9 primers, and UPM and TR-8 primers. A 0.4 kb fragment (5'-RACE; 5'-DNA end) and a 0.8 kb DNA (3'-RACE; 3'-DNA end) were amplified by PCR. Both DNA fragments were subcloned into pCR4 vector and transformed into *E. coli* TOPO10. The nucleotide sequences of these inserts were determined in both strands. Sequence analysis revealed that the combined sequences covered an open reading frame of a putative TcTR cDNA (1273 bp, EMBL accession no. EF017814).

**Bioinformatics Analysis.** The blast program was used to search homologous protein sequences in the nonredundant database at the National Center for Biotechnology Information, National Institutes of Health (<http://www.ncbi.nlm.nih.gov/>). Multiple alignments were constructed using the ClustalW2 program (<http://www.ebi.ac.uk/Tools/clustalw2/index.html>). Structural modeling was carried out by using the SWISS-MODEL program (<http://swissmodel.expasy.org/>

<http://www.expasy.org/spdbv/>) (24). The modeling data was then superimposed by DeepView Swiss-PdbViewer v3.7 (<http://www.expasy.org/spdbv/>) (24).

**Subcloning of the TcTR cDNA into an Expression Vector.** The coding region of the TcTR cDNA was amplified by using two gene-specific primers. The 5' upstream primer contains the *EcoRI* recognition site (5' GAATTCG ATG GCT CCA ACG ACG AAT GGA G 3') and the 3' downstream primer contains a 6His-tag and *EcoRI* recognition site (5' GAATTCCTA GTG GTG GTG GTG GTG GTG CTC CTC GAC ACC CTC TTC CTC 3'). Using 0.2  $\mu$ g of TcTR cDNA as a template and 10 pmole of each 5' upstream and 3' downstream primers, we amplified a 1.0 kb fragment by PCR. The fragment was ligated into pCR4 and transformed into *E. coli*. The recombinant plasmid was isolated and digested with *EcoRI*. The digestion products were separated on a 0.8% agarose gel. The ~1.0 kb insert DNA was gel purified and subcloned into the *EcoRI* site of pYEX-S1 expression vector (Clontech) and introduced into *Saccharomyces cerevisiae* (trp<sup>-</sup> ura<sup>-</sup>). The transformed yeast cells were selected by YNBDT (0.17% yeast nitrogen base, 0.5% ammonium sulfate, and 2% glucose) agar plates containing 20  $\mu$ g Trp/mL. The presence of TcTR cDNA in the selected transformants was verified by PCR using gene specific flanking primers. The recombinant TcTR protein was expressed in yeast in YPD medium (1% yeast extract, 2% peptone, and 2% glucose). Functional recombinant TcTR protein was identified by an activity assay as described below.

**Expression and Purification of the Recombinant TcTR.** The transformed yeast containing the TcTR gene was grown at 30 °C in 200 mL of YPD medium for 5 days. The cells were harvested and soluble proteins extracted in PBS with glass beads as described before (25). The recombinant TcTR was purified by Ni-NTA affinity chromatography (elution buffer: 0.3 $\times$  PBS containing 100 mM imidazole) as per the manufacturer's instructions (Qiagen). The purified protein was checked by 10% SDS-PAGE and native-PAGE. Proteins on gel were detected by staining with Coomassie brilliant blue. Protein concentration was determined by Bio-Rad Protein Assay Kit using bovine serum albumin as a standard.

**Molecular Mass Determination by ESI Q-TOF.** The purified TcTR (0.4 mg/mL) in 0.003 $\times$  PBS containing 0.05 mM imidazole and 0.05% glycerol was shipped to Yao-Hong Biotechnology Company (Taiwan) for molecular mass determination using ESI Q-TOF (electrospray ionization quadrupole-time-of-flight) mass spectrometry (Micromass, Manchester, England).

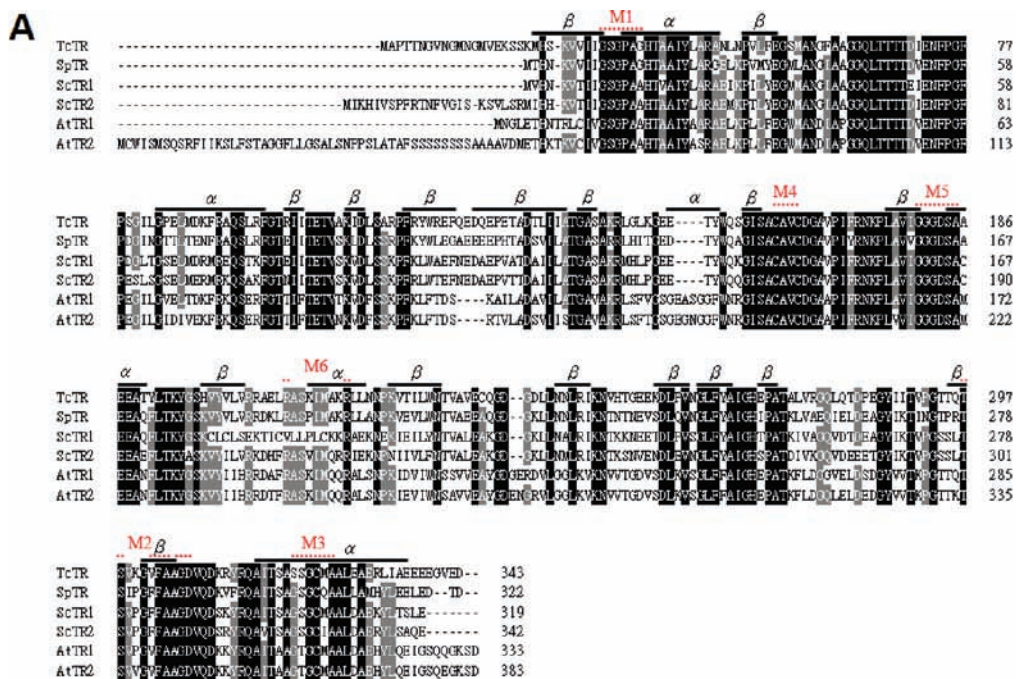
**Detection of TcTR Activity via the DTNB Assay.** The activity of TcTR was determined by monitoring the NADPH-dependent reduction of DTNB [5,5-dithiobis(2-nitrobenzoic acid)] as described elsewhere (26) with some modifications. The assay mixture (100  $\mu$ L) contained 75 mM potassium phosphate buffer (pH 7.4), 0.2 mM EDTA, 1.5 mM DTNB, 0.2 mM NADPH, and 0.74–1.9  $\mu$ g of purified TcTR. The absorbance at 412 nm was recorded for 1.0 min. Nonenzymatic reduction of DTNB by NADPH was measured in a separate cuvette, and the absorbance increment over that of the blank activity was taken for TcTR activity. The absorbance coefficient of TNB at 412 nm is  $\epsilon = 13.6 \text{ mM}^{-1} \text{ cm}^{-1}$ . Two moles of 5-thio-2-nitrobenzoic acid (TNB) are formed for 1 mol of NADPH oxidized.

**Enzyme Characterization.** The enzyme sample (1.9  $\mu$ g for each treatment) was tested for effect under various conditions.

1. **Thermal Effect.** The enzyme sample was heated at 60 °C for 2, 4, 8, or 16 min. Three aliquots of each sample were analyzed by electrophoresis onto a 10% SDS gel and a 10% native gel, and the changes in TcTR activity determined.

2. **pH Effect.** The purified TcTR was adjusted to the desired pH by adding a half volume of buffer with different pH values: 0.2 M citrate buffer (pH 2.5 or 4.0), 0.2 M potassium phosphate buffer (pH 6.0 or 8.0), or 0.2 M CAPS buffer (pH 10.0 or 11.0). Each sample was incubated at 37 °C for 1 h to determine the changes in TcTR activity.

3. **Imidazole Effect.** During protein purification, the TR enzyme was eluted with imidazole. Thus, the effect of imidazole on protein activity was examined. Imidazole was added to the enzyme sample to the levels of 0.2 or 0.4 M and incubated at 37 °C for 1 h to determine the changes in TcTR activity.



**B**

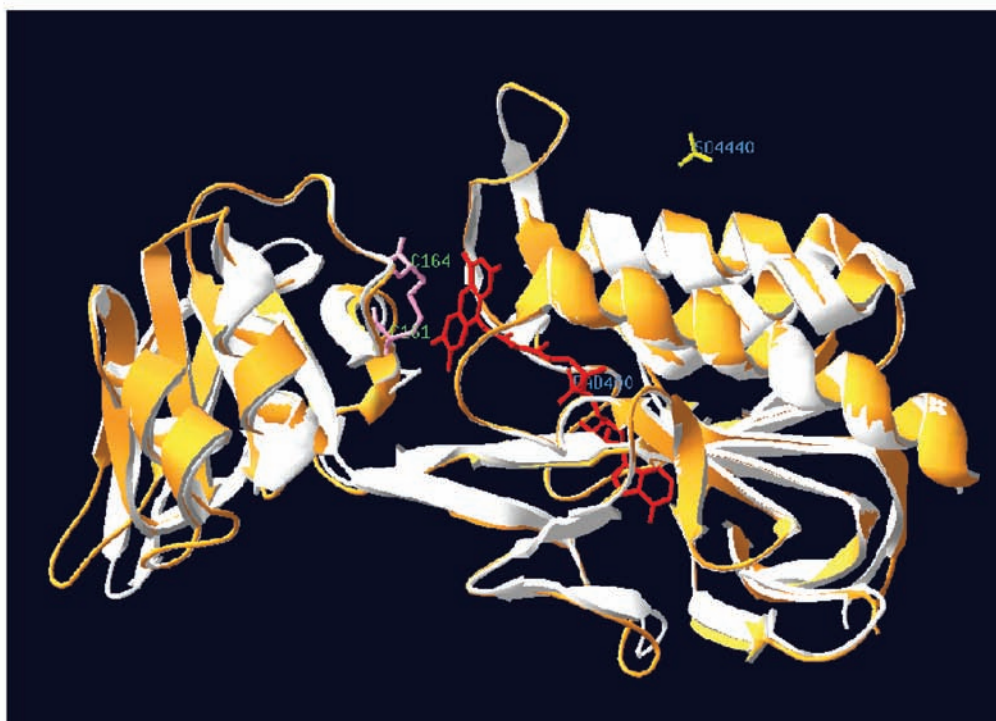


**Figure 1.** Alignment of the amino acid sequences of TcTR with other organisms and predicted 3-D homology structure. **(A)** Sequence alignment: TcTR (this study), SpTR (*Schizosaccharomyces pombe*), ScTR1 (*Schizosaccharomyces cerevisiae*), ScTR2 (*Schizosaccharomyces cerevisiae*), AtTR1 (*Arabidopsis thaliana*), and AtTR2 (*Arabidopsis thaliana*). Identical amino acids in all sequences are shaded black, and conservative replacements are shaded gray. M1–M6 denote putative active site motifs and cofactor binding sites. Protein secondary structure was predicted by the SWISS-MODEL program and represented as  $\alpha$  helices and  $\beta$  strands. **(B)** A 3-D homology structure of TcTR. The structure of TcTR was created on the basis of the known structure of *Arabidopsis thaliana* NADPH dependent thioredoxin reductase (PDB code 1VDC) and was superimposed to obtain better structure alignment via SWISS-MODEL and DeepView Swiss-PdbViewer v3.7 programs. Superimposition of TcTR (orange color) and *Arabidopsis thaliana* NADPH dependent thioredoxin reductase (white) was shown by using protein solid ribbons. Pink denotes the active site (C<sup>161</sup>AVC<sup>164</sup>). Red denotes FAD.

4. *Susceptibility to Proteolytic Digestion.* The enzyme was incubated with one-tenth its weight of trypsin or chymotrypsin at pH 8.0 at 37 °C for a period of 5, 10, 20, or 40 min. The sample was removed at various time intervals for activity analysis.

**Kinetic Studies.** TcTR activities were tested at 25 °C by monitoring the reduction of DTNB at A<sub>412</sub>. The kinetic properties of TcTR (0.75  $\mu$ g) in a total volume of 100  $\mu$ L were determined using various concentrations of DTNB (0.5 to 8 mM) with the fixed amount of

0.2 mM NADPH. The  $K_m$ ,  $V_{max}$ , and  $K_{cat}$  were calculated from Lineweaver–Burk plots.

## RESULTS

**Cloning and 3-D Homologous Structure of TcTR.** A putative TcTR cDNA clone was identified using the consensus pattern and sequence homology to the published TRs. The TcTR cDNA (1273 bp, EMBL accession no. EF017814) contains an open reading frame which encodes a protein of 343 amino acid residues with a predicted molecular mass of 37 kDa. **Figure 1A** shows the amino acid sequence alignment of the TcTR with TR from several sources. The TcTR shared 74, 68, 69, 61, and 62% sequence identity with TR from *Schizosaccharomyces pombe* (SpTR, accession no. AAN01228), *Saccharomyces cerevisiae* (ScTR1, accession no. AAA64747), *Saccharomyces cerevisiae* (ScTR2, accession no. P38816), *Arabidopsis thaliana* (AtTR1, accession no. Q39243), and *Arabidopsis thaliana* (AtTR2, accession no. Q39242), respectively.

A structure of TcTR was created on the basis of the known structure of *Arabidopsis thaliana* NADPH dependent thioredoxin reductase (AtTR1, PDB code 1VDC) and was superimposed to obtain better structure alignment (**Figure 1B**) via SWISS-MODEL and DeepView Swiss-PdbViewer v3.7 programs. The amino acid sequences of TcTR and the AtTR1 share 61% homology.

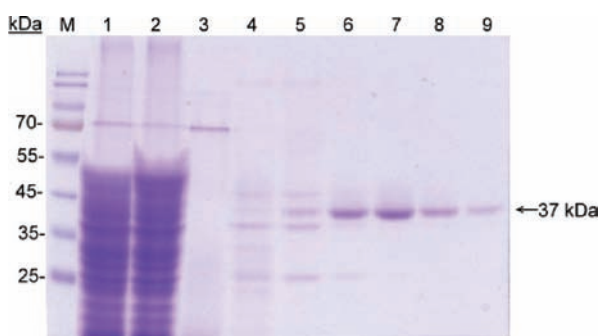


**Figure 2.** Purification of the recombinant TcTR. Twelve milliliters of crude extract was obtained from 200 mL of culture. Ten microliters of each sample was performed on a 10% SDS–PAGE followed by Coomassie blue staining. Lanes: 1, crude extract; 2, flow through; 3, wash; 6–9, eluted TcTR fractions.

The secondary structure was predicted by the same program and represented as  $\alpha$  helices and  $\beta$  strands (**Figure 1A**). The crystal structure of TR from *Arabidopsis thaliana* has been determined at 2.5 Å resolution and its active site motif ( $C^{161}AVC^{164}$ ), FAD, and NADPH binding sites identified (24). These sites are conserved in the TcTR. The putative N-terminal FAD-binding domain is represented by the glycine-rich motif GSGPAG (position 29–34, M1). The putative central NADPH-binding domain may be believed to involve the redox-active disulfide between  $C^{161}$  and  $C^{164}$  (CAVC, M4) and another glycine-rich motif GGGDSA (position 180–185, M5). We also found the basic residues  $R^{204}$  and  $R^{209}$  (M6) that presumably interact with the 2'-phosphate group of NADP. The putative C-terminal FAD-binding domain involves the TS (position 297–298), VFA (position 302–304), GD (position 306–307, M2), and SSGCMA (position 321–326, M3) that may be involved in electron flow between NADPH and oxidized glutathione via FAD as in the case of TR from *Arabidopsis thaliana* (24).

**Expression and Purification of the Recombinant TcTR.** The cDNA was introduced into a yeast expression system as described in the Materials and Methods section. The recombinant TcTR protein was expressed, and the total cellular proteins were analyzed by SDS–PAGE (**Figure 2**, lane 1). The His-tagged TcTR fusion protein was purified by Ni-NTA affinity chromatography. The TcTR was eluted as a single band with an apparent molecular mass of 37 kDa (**Figure 2**, lanes 6–9). The mass is consistent with the monomeric TR. An ESI Q-TOF of the TcTR under the conditions of  $0.003\times$  PBS containing 0.05 mM imidazole and 0.05% glycerol reveals that the protein exists as a monomer. When using native PAGE to check for TcTR, we show only one protein band in **Figure 3B**. Taken together, these results suggest that the enzyme is monomeric in nature. The yield of the purified TcTR was 2.25 mg per 250 mL of culture.

**Characterization of the Purified TcTR.** The TcTR enzyme activity appears to be stable at 60 °C for a short period. The enzyme inactivation kinetics at 60 °C fit the first-order inactivation rate equation  $\ln(E_t/E_0) = -K_d t$ , where  $E_0$  and  $E_t$  represent the original activity and the residual activity after heating for time  $t$ , respectively. The thermal inactivation rate constant ( $K_d$ ) calculated for the enzyme at 60 °C was  $5.37 \times 10^{-2} \text{ min}^{-1}$ , and the half-life of inactivation was 12.9 min (**Figure 3C**). The TcTR had an optimal pH at 8.0 as shown in **Figure 4A**. The TcTR

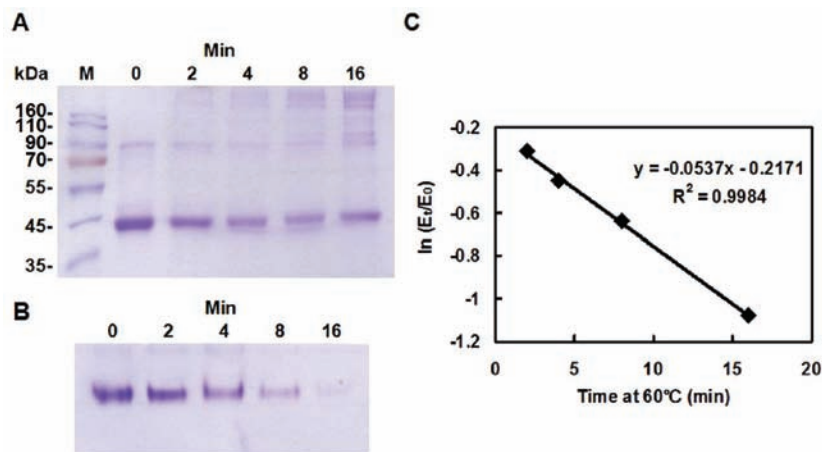


**Figure 3.** Effect of temperature on purified TcTR. The enzyme samples heated at 60 °C for various time intervals were analyzed by (A) 10% SDS–PAGE and (B) 10% native PAGE. Both were stained for proteins (1.5  $\mu\text{g}/\text{lane}$ ). Lanes 1 to 5 were purified TcTR heated for 0, 2, 4, 8, 16 min, respectively. (C) Plot of thermal inactivation kinetics. The effect of temperature was determined by the activity assay.  $E_0$  and  $E_t$  are original activity and residual activity, respectively, after being heated for different time intervals. The data are the mean of three independent experiments.

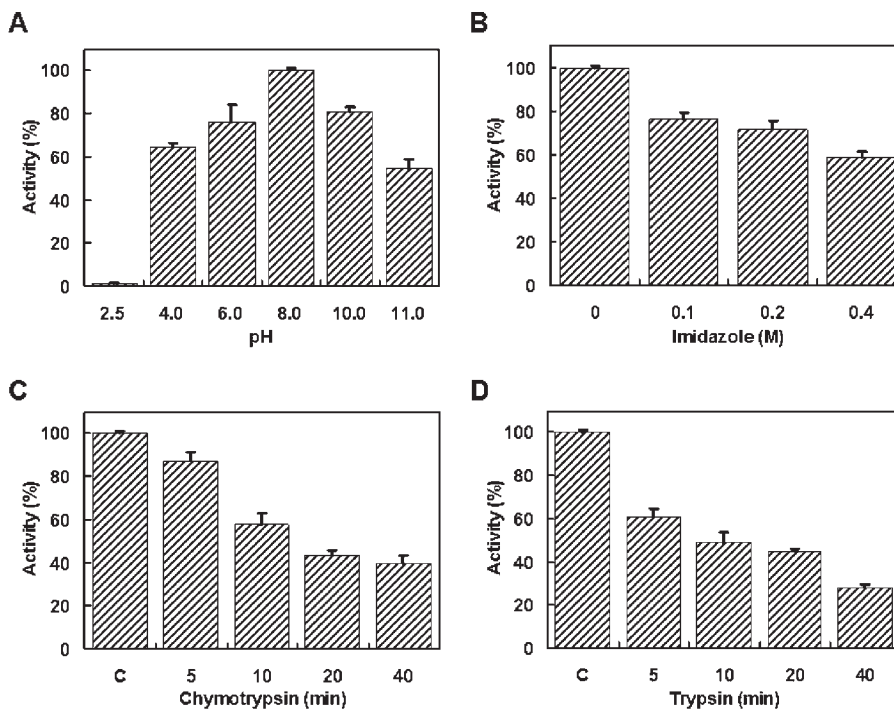


**Figure 4.** Effect of pH, imidazole, chymotrypsin, and trypsin on the activity of purified TcTR (1.9  $\mu\text{g}/\text{lane}$ ). (A) The enzyme samples were incubated in buffers with different pH values at 37 °C for 1 h and then subjected to the activity assay. (B) The enzyme samples were incubated with imidazole of different concentrations at 37 °C for 1 h and then subjected to the activity assay. (C) The enzyme samples were incubated with chymotrypsin at 37 °C for various time intervals and then subjected to the activity assay. (D) The enzyme samples were incubated with trypsin at 37 °C for various time intervals and then subjected to the activity assay. The data are the mean of three independent experiments.

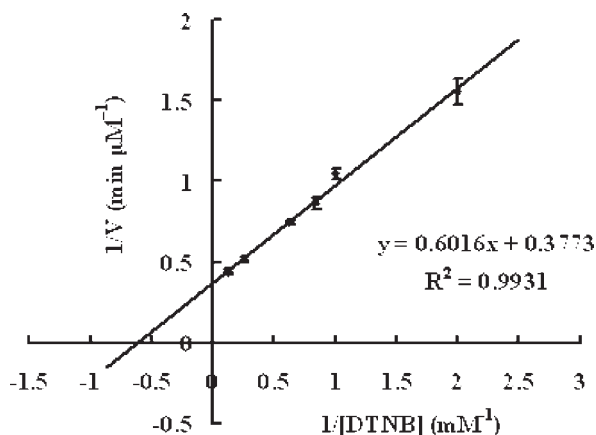


**Figure 5.** Double-reciprocal plot of TcTR activity at varying concentrations of DTNB. The initial rate of the enzymatic reaction was measured at 0.2 mM NADPH with the DTNB concentration varied from 0.5 to 8 mM. The  $K_m$ ,  $V_{max}$ , and  $K_{cat}$  were calculated from the plots.

activity dropped 20–40% with increasing concentrations of imidazole from 0.1 to 0.4 M (Figure 4B). The enzyme retained 40% activity after treatment with chymotrypsin (Figure 4C) or trypsin (Figure 4D) for 40 min. The results suggested that the TcTR may have a rigid structure and that the potential cleavage sites were not readily accessible by the enzymes under the reaction conditions. 1-Cys peroxiredoxin was used as a positive control in protease digestion. The peroxiredoxin was degraded within 20 min of treatment with either trypsin or chymotrypsin (results not shown).

**Kinetic Studies of the TcTR.** As shown in Figure 5, the Lineweaver–Burk plot of the velocity ( $1/V$ ) against  $1/[\text{DTNB}]$  gave  $K_m = 1.59$  mM,  $V_{max} = 2.65$   $\mu\text{M}/\text{min}$ , and  $K_{cat} = 13.08$   $\text{min}^{-1}$ .

**Table 1.** Kinetic Characterization of TcTR and Other Published TRs<sup>a</sup>

enzyme	$K_m$ ( $\mu\text{M}$ )	$K_{cat}$ ( $\text{S}^{-1}$ )	$K_{cat}/K_m$ ( $\text{M}^{-1} \times \text{s}^{-1}$ )
TcTR <sup>b</sup>	1590	13	$8.0 \times 10^3$
hTR <sup>b</sup>	400 <sup>c</sup>	67 <sup>c</sup>	$1.7 \times 10^5$
PfTR <sup>b</sup>	1090 <sup>d</sup>	7 <sup>d</sup>	$6.4 \times 10^3$

<sup>a</sup> The kinetic parameter was determined as described in Materials and Methods. The  $K_m$  value for dithionitrobenzoate (DTNB) was determined at 0.5–8 mM DTNB and 0.2 mM NADPH. Data represent the mean ( $\pm$ SE) of three separate experiments. <sup>b</sup> These values are from recombinant expressed enzymes. <sup>c</sup> These values are from the literature [hTR (30)]. <sup>d</sup> These values are from the literature [PfTR (31)].

## DISCUSSION

This study reported the cloning and expression of TcTR from *T. camphorata*. The biologically active form of TcTR has been successfully expressed in yeast.

Many oxidoreductases such as glutathione reductase (27) and dehydroascorbate reductase (28), among others, possess Cys residues that are important in catalyzing redox reactions. As seen in the sequence and predicted 3-D structure of TcTR (Figure 1), the enzyme contains two conserved Cys residues at positions 161 and 164. It is believed that the two Cys residues participate in the transfer of electrons from NADPH in the Trx reduction as reported by Dai et al. (24). The TcTR exists predominantly as a monomer as determined by SDS–PAGE (Figure 2), native PAGE (Figure 3), and ESI Q-TOF. Thus, Cys161 and Cys164 are not expected to form intermolecular disulfide bonds.

The TcTR protein contains several potential trypsin cleavage sites and potential chymotrypsin-high specificity cleavage sites or chymotrypsin-low specificity cleavage sites. However, the native enzyme appeared to be resistant to digestion by trypsin and chymotrypsin even at a high enzyme/substrate (w/w) ratio of 1/10 (Figure 4C and D). This may be due to its rigid or compact structure and limited accessibility of the enzymes to the potential

cleavage sites under the reaction conditions. It has been reported that proteins were attacked by trypsin less readily in their native state than when they are denatured (29).

As shown in **Table 1**, TcTR has a higher  $K_m$  value (1590  $\mu\text{M}$ ) to reduce DTNB than hTR (400  $\mu\text{M}$ ) from human placenta and PfTR (1090  $\mu\text{M}$ ) from *Plasmodium falciparum*. A reasonable explanation for the discrepancy in their  $K_m$  values is that *T. camphorata* grows in dark, moist environments devoid of harsh environments such as UV light and encounters lower oxidative stress. Therefore, TcTR cannot use lower concentrations of NADPH to perform reduction reactions for protection against oxidative stress.

## LITERATURE CITED

- Powis, G.; Mustacich, D.; Coon, A. The role of the redox protein thioredoxin in cell growth and cancer. *Free Radical Biol. Med.* **2000**, *29*, 312–322.
- Becker, K.; Gromer, S.; Schirmer, R. H.; Muller, S. Thioredoxin reductase as a pathophysiological factor and drug target. *Eur. J. Biochem.* **2000**, *267*, 6118–6125.
- Mitsui, A.; Hamuro, J.; Nakamura, H.; Kondo, N.; Hirabayashi, Y.; Ishizaki-Koizumi, S.; Hirakawa, T.; Inoue, T.; Yodoi, J. Overexpression of human thioredoxin in transgenic mice controls oxidative stress and life span. *Antioxid. Redox Signaling* **2002**, *4*, 693–696.
- Williams, C. H., Jr. Mechanism and structure of thioredoxin reductase from *Escherichia coli*. *FASEB J.* **1995**, *9*, 1267–1276.
- Chae, H. Z.; Chung, S. J.; Rhee, S. G. Thioredoxin dependent peroxide reductase from yeast. *J. Biol. Chem.* **1994**, *269*, 27670–27678.
- Tamura, T.; Stadtman, T. C. A new selenoprotein from human lung adenocarcinoma cells: purification, properties, and thioredoxin reductase activity. *Proc. Natl. Acad. Sci. U.S.A.* **1996**, *93*, 1006–1011.
- Gladyshev, V. N.; Jeang, K. T.; Stadtman, T. C. Selenocysteine, identified as the penultimate C-terminal residue in human T-cell thioredoxin reductase, corresponds to TGA in the human placental gene. *Proc. Natl. Acad. Sci. U.S.A.* **1996**, *93*, 6146–6151.
- Arscott, L. D.; Gromer, S.; Schirmer, R. H.; Becker, K.; Williams, C. H., Jr. The mechanism of thioredoxin reductase from human placenta is similar to the mechanisms of lipoamide dehydrogenase and glutathione reductase and is distinct from the mechanism of thioredoxin reductase from *Escherichia coli*. *Proc. Natl. Acad. Sci. U.S.A.* **1997**, *94*, 3621–3626.
- Zang, M.; Su, Q. *Ganoderma camphoratum*, a new taxon in genus *Ganoderma* from Taiwan. *China Acta Bot. Yunnanica* **1990**, *12*, 395–396.
- Chang, T. T.; Chou, W. N. *Antrodia cinnamomea* sp. nov. on *Cinnamomum kanehirai* in Taiwan. *Mycol. Res.* **1995**, *99*, 756–758.
- Wu, S. H.; Ryvarden, L.; Chang, T. T. *Antrodia camphorata* (“niu-chang-chih”), new combination of a medicinal fungus in Taiwan. *Bot. Bull. Acad. Sin.* **1997**, *38*, 273–275.
- Wu, S. H.; Yu, Z. H.; Dai, Y. C.; Chen, C. T.; Su, C. H.; Chen, L. C.; Hsu, W. C.; Hwang, G. Y. *Taiwanofungus*, a polypore new genus. *Fung. Sci.* **2004**, *19*, 109–116.
- Chiu, H. H. Phylogenetic analysis of *Antrodia* species and *Antrodia camphorata* inferred from internal transcribed spacer region. *Antonie van Leeuwenhoek* **2007**, *91*, 267–276.
- Ao, Z. H.; Xu, Z. H.; Lu, Z. M.; Xu, H. Y.; Zhang, X. M.; Dou, W. F. Niu-chang-chih (*Antrodia camphorata*) and its potential in treating liver diseases. *J. Ethnopharmacol.* **2009**, *121*, 194–212.
- Geethangili, M.; Tzeng, Y. M. Review of pharmacological effects of *Antrodia camphorata* and its bioactive compounds. *eCAM* **2009**, nep108.
- Wen, L.; Huang, H. M.; Juang, R. H.; Lin, C. T. Biochemical characterization of l-Cys peroxiredoxin from *Antrodia camphorata*. *Appl. Microbiol. Biotechnol.* **2007**, *73*, 1314–1322.
- Huang, J. K.; Ken, C. F.; Huang, H. M.; Lin, C. T. Biochemical characterization of a novel 2-Cys peroxiredoxin from *Antrodia camphorata*. *Appl. Microbiol. Biotechnol.* **2007**, *74*, 84–92.
- Liau, Y. J.; Wen, L.; Shaw, J. F.; Lin, C. T. A highly stable cambialistic-superoxide dismutase from *Antrodia camphorata*: expression in yeast and enzyme properties. *J. Biotechnol.* **2007**, *131*, 84–91.
- Ken, C. F.; Chen, H. T.; Chang, R. C.; Lin, C. T. Biochemical characterization of a catalase from *Antrodia camphorata*: expression in *Escherichia coli* and enzyme properties. *Bot. Stud.* **2008**, *49*, 119–125.
- Huang, C. Y.; Ken, C. F.; Wen, L.; Lin, C. T. An enzyme possessing both glutathione-dependent formaldehyde dehydrogenase and S-nitrosoglutathione reductase from *Antrodia camphorata*. *Food Chem.* **2009**, *112*, 795–802.
- Chen, H. T.; Lin, C. Y.; Ken, C. F.; Wen, L.; Lin, C. T. Putative phospholipid hydroperoxide glutathione peroxidase from *Antrodia camphorata*. *Food Chem.* **2009**, *115*, 476–482.
- Ken, C. F.; Lin, C. Y.; Jiang, Y. C.; Wen, L.; Lin, C. T. Cloning, expression and characterization of an enzyme possesses both glutaredoxin and dehydroascorbate reductase activity from *Taiwanofungus camphorata*. *J. Agric. Food Chem.* **2009**, *57*, 10357–10362.
- Liau, Y. J.; Chen, Y. T.; Lin, C. Y.; Huang, J. K.; Lin, C. T. Characterization of 2-Cys peroxiredoxin isozyme (Prx1) from *Taiwanofungus camphorata* (Niu-chang-chih): expression and enzyme properties. *Food Chem.* **2010**, *119*, 154–160.
- Dai, S.; Saarinen, M.; Ramaswamy, S.; Meyer, Y.; Jacquot, J. P.; Eklund, H. Crystal structure of *Arabidopsis thaliana* NADPH dependent thioredoxin reductase at 2.5 Å resolution. *J. Mol. Biol.* **1996**, *264*, 1044–1057.
- Ken, C. F.; Hsiung, T. M.; Huang, Z. X.; Juang, R. H.; Lin, C. T. Characterization of Fe/Mn-superoxide dismutase from diatom *Thalassiosira weissflogii*: cloning, expression, and property. *J. Agric. Food Chem.* **2005**, *53*, 1470–1474.
- Jeon, S. J.; Ishikawa, K. Identification and characterization of thioredoxin and thioredoxin reductase from *Aeropyrum pernix* K1. *Eur. J. Biochem.* **2002**, *269*, 5423–5430.
- Chen, C. J.; Huang, C. Y.; Huang, J. K.; Lin, C. Y.; Lin, C. T. Cloning, expression and purification of a functional glutathione reductase from sweet potato (*Ipomoea batatas* [L.] Lam): kinetic studies and characterization. *J. Agric. Food Chem.* **2009**, *57*, 4403–4408.
- Jiang, Y. C.; Huang, C. Y.; Wen, L.; Lin, C. T. Dehydroascorbate reductase cDNA from sweet potato (*Ipomoea batatas* [L.] Lam): expression, enzyme properties, and kinetic studies. *J. Agric. Food Chem.* **2008**, *56*, 3623–3627.
- Haurowitz, F.; Tunca, M.; Schwerin, P.; Göksu, V. The action of trypsin on native and denatured proteins. *J. Biol. Chem.* **1945**, *157*, 621–625.
- Gromer, S.; Arscott, L. D.; Williams, C. H.; Schirmer, R. H.; Becker, K. Human placenta thioredoxin reductase. Isolation of the selenoenzyme, steady state kinetics, and inhibition by therapeutic gold compounds. *J. Biol. Chem.* **1998**, *273*, 20096–20101.
- Müller, S.; Gilberger, T. W.; Färber, P. M.; Becker, K.; Schirmer, R. H.; Walter, R. D. Recombinant putative glutathione reductase of *Plasmodium falciparum* exhibits thioredoxin reductase activity. *Mol. Biochem. Parasitol.* **1996**, *80*, 215–219.

---

Received for review January 19, 2010. Revised manuscript received March 7, 2010. Accepted March 11, 2010. This work was partially supported by the National Science Council of the Republic of China, Taiwan under Grant NSC 97-2313-B-019-001-MY3 to C-T.L.